CIRP Annals - Manufacturing Technology 69 (2020) 341–344

Contents lists available at ScienceDirect

CIRP Annals - Manufacturing Technology

journal homepage: https://www.editorialmanager.com/CIRP/default.aspx

Development and evaluation of a dynamic powder splitting system for the directed energy deposition (DED) process

Masakazu Soshi[a,*], Curtis Yau[a], Ryohei Kusama[b]

[a] Department of Mechanical and Aerospace Engineering, University of California, Davis, One Shields Avenue, Davis, CA 95616, United States
[b] DMG Mori Co., Ltd., 2-35-16 Meieki, Nakamura-ku, Nagoya, Aichi 450-0002, Japan

Submitted by Prof. Yotaro Hatamura (1), Hatamura Institute for the Advancement of Technology, Tokyo, Japan

ARTICLE INFO

Article history:
Available online 17 May 2020

Keywords:
Additive manufacturing
Design
Powder flow control

ABSTRACT

A dynamic powder splitting system (DPSS) was developed to overcome a slow powder flow rate (PFR) response in conventional powder delivery systems used in the Directed Energy Deposition (DED) additive manufacturing process. Complementary to the main powder delivery system, the DPSS uses a custom valve to split powder flow and cyclone separator to redirect powder flow that is not used in the cladding process. Its potential applications are compensation for clad height inconsistencies caused by machine feed rate errors and increase of powder usage efficiency via a powder recycling system. Various tests were performed to verify performance and cladding.

1. Introduction

Directed energy deposition (DED) is an additive manufacturing (AM) process capable of creating complex metal parts. The working principle of DED involves directing energy (e.g. laser) towards a feedstock (e.g. fine metal powder) to melt the material onto a substrate. As the energy source moves the previously deposited material (i.e. clad) solidifies, as shown in Fig. 1. The feedstock is conveyed to the clad using an inert gas which also acts to prevent oxidation during the DED process [1]. This research focuses on controlling the flow rate of metal powder used in DED to advance the overall manufacturing process.

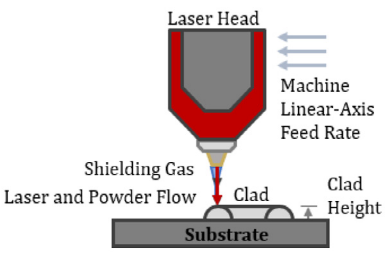

Fig. 1. DED process involving fine metal powder and laser.

Previous research shows that the energy flux, *EF*, as defined in (1), is related to the clad width while clad height is mainly dependent on powder flux, *PF*, as defined in (2) [2–4]. For *EF*, laser power, *P*, is inversely proportional to the product of laser feed rate, *F*, and laser spot diameter, *d*. For *PF*, the powder flow rate, *PFR*, is inversely proportional to the product of *F* and *d*.

$$EF = \frac{P}{F \cdot d} \quad (1)$$

$$PF = \frac{PFR}{F \cdot d} \quad (2)$$

1.1. Motivation

There are three motivations behind quickly controlling PFR: dynamic compensation of powder flow, powder waste reduction, and productivity improvements using advanced process controls.

First, inconsistent clad geometry is often caused by feed rate errors of a computer numerical control (CNC) machine's servo motors when sharply changing axes directions such as at corners. Feed rate accelerations and decelerations cause overbuilds due to decrease in laser feed rate, as understood by (2). Second, interlayer dwells are often used to allow deposited material to cool and accumulated energy to dissipate before deposition of the next layer. Energy accumulation is important to consider because it, along with *EF*, affect the final clad width. Typically, powder flow is not stopped during dwelling due to slow powder feeding system response times and the powder expelled during dwelling is wasted. If a system can be developed to quickly close powder flow during dwells, it would be monetarily beneficial as metal powders are very expensive. Third, new deposition approaches can be achieved using sophisticated powder and energy controls.

* Corresponding author.
E-mail address: msoshi@ucdavis.edu (M. Soshi).

https://doi.org/10.1016/j.cirp.2020.04.048
0007-8506/

1.2. Problem and objective

The most common powder feeding system in DED machines is a hopper – disk system where a hopper pressurized with inert gas empties feed stock onto a rotating disk. Powder on the disk is conveyed to an orifice connected to tubing where the escaping pressurized gas creates a vacuum that sends the powder into the tubing. The tubing is connected to the laser head where the powder and carrier gas are directed through a nozzle to the meltpool. Although capable of fine PFR control, the hopper – disk delivery system has slow response to PFR changes (on the order of several seconds) due to the long distance from it to the laser head. This hopper – disk placement is due to its large size. Typically, the user is advised to wait 10 s after changing the PFR to ensure steady state PFR at the nozzle. Thus, the dynamic powder splitting system (DPSS) must be implemented as close to the laser head as possible in series with the hopper – disk powder delivery system to achieve faster PFR time response.

The two main objectives of the DPSS are: (1) to switch between different steady-state PFRs in $\leq$ 0.5 s and (2) to recycle powder flow not used in the deposition process. In addition to these objectives, the system should also:

- modulate powder flow while keeping carrier gas flow constant so minimal oxidation occurs during cladding
- maintain stable PFR
- be capable of long industrial operational hours.

Previously, a similar system was developed via a solenoid valve to control powder flow [5]. However, with many small moving parts within, the design may be extremely susceptible to failure by seizure and wear. Additionally, the system in [5] requires a supplemental gas source which is not economically preferable.

2. Dynamic powder splitting system design

The proposed DPSS design involves two main components: a valve for moderating powder flow and a cyclone separator to recycle both the powder and carrier gas used to convey the powder, Fig. 2. The valve is placed downstream of the existing hopper – disk powder delivery system and moderates powder between the laser head and cyclone separator. The cyclone separator connects to a container that stores unused powder and reroutes the carrier gas to the laser head, allowing carrier gas flow to remain constant without an additional gas source.

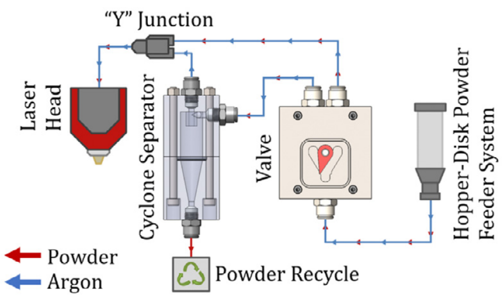

Fig. 2. Valve and cyclone separator setup for DPSS.

The system was designed to be tested in a DMG Mori Lasertec 65 3D hybrid CNC machine equipped with a GTV hopper – disk type powder feeding system.

2.1. Valve design

The valve design consists of one inlet and two outlets. One outlet directs powder towards the laser head and the other outlet directs powder towards the cyclone separator. Internal channels were designed so that powder flow may be manipulated smoothly, as shown in Fig. 3(a). The channel cross sections were designed to be as close as possible to the area of the 4 mm ID tubing used in the existing powder system. A P20 tool steel powder splitter with 0.25 mm radius tip is used to divert powder flow. A Sanyo Denki R2AA06010F AC 0.318 N-m rated servomotor with a mechanical and electrical time constant of 1.2 ms and 2.0 ms, respectively, is used to actuate the splitter that controls the amount of powder flowing to each valve outlet. The powder splitter is capable of approximately 30° of movement. The metal powder used for this research is 316 L stainless steel with particles ranging from 45–160 μm in diameter.

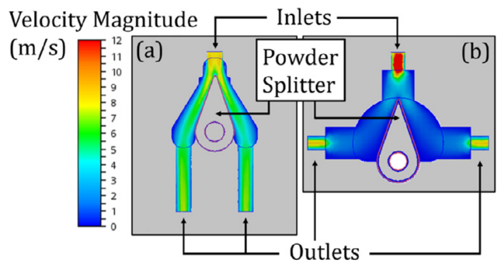

Fig. 3. CFD simulation of (a) current and (b) initial valve design.

To minimize powder stagnation and saltation in the valve a computational fluid dynamics (CFD) simulation of carrier gas flow through the valve was performed, Fig. 3(a). A 6 l/min volumetric flow rate boundary condition was chosen for the inlet and 500 Pa pressure boundary condition was chosen for the outlets. The geometry was optimized by minimizing the areas of low velocity (i.e. 0–1 m/s) where powder stagnation was observed during testing of the initial design, Fig. 3(b).

2.2. Cyclone separator design

The cyclone separator was chosen as the powder recycling mechanism because it is capable of both powder collection and carrier gas recovery. The recovered carrier gas can be rerouted to the laser head to ensure constant flow out of the nozzle; no supplementary carrier gas is required.

The 2D2D cyclone by Shepherd and Lapple is very efficient for small particles [6]. A *Dc* value of 16 mm was used so that the inlets and outlets of the cyclone separator would be the same size as the tubing used in the existing powder system. The *Hc* and *Bc* parameters from [7] were modified into circular cross-section values to match the powder system tubing. Dimensions of the final cyclone separator are shown in Fig. 4.

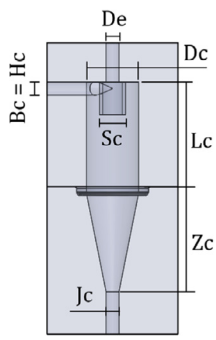

2D2D Cyclone Design
Dimensions with Dc = 16 mm

Parameter	Design Ratio	Dimension [mm]
Bc = Hc	Dc/4	4
Sc	Dc/8	2
De	Dc/2	8
Lc	2Dc	32
Zc	2Dc	32
Jc	Dc/4	4

Fig. 4. 2D2D Cyclone Separator Design by Shepherd and Lapple [7].

The efficiency of a cyclone separator is particle size dependent [8]. Eq. (3) can be used to estimate the smallest particle diameter, d_{pc}, that a cyclone separator can collect with $\geq$50% efficiency. Particles larger than d_{pc} are collected with a higher efficiency. In (3), μ_g is the viscosity of the fluid, W_I is the inlet width, N_e is the number of effective turns (3.05 for a 2D2D cyclone), V_i is the velocity fluid at the inlet, and ρ_p is the particle density [8]. For velocities <8 m/s, the maximum fluid velocity expected, d_{pc} is significantly smaller than 45 μm, Fig. 5.

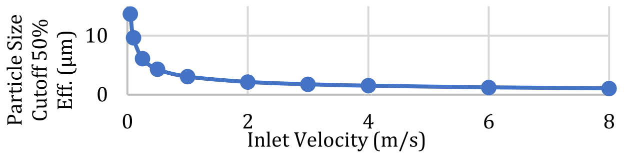

Fig. 5. Cutoff diameter of particle collected with at least 50% efficiency with inlet velocities ranging from 0.1 m/s to 8.0 m/s.

$$d_{pc} = \left[\frac{9\mu_g W_I}{2\pi N_e V_i \rho_p}\right]^{\frac{1}{2}} \tag{3}$$

3. Performance testing

3.1. Stability and PFR resolution

Powder flow stability tests were performed using an electronic mass scale with a sampling rate of 10.4 Hz. Powder mass was measured from the hopper – disk system alone and from the valve in 1° increments. Standard deviation from the average PFR measured from the mass vs. time data was used to determine stability. The standard deviation from the powder – disk system was found to be 2.3% of the maximum PFR, while it was found to be 3.3% from the valve when fully opened. This amount is negligible when compared to the maximum PFR. Additionally, as the opening to the nozzle decreases (i.e. goes towards 30°), the standard deviation gradually decreases as well, implying that there is little to no increase of powder flow error.

PFR resolution tests were performed for every 1° increment of travel of the powder splitter. Tests were initially performed with the existing hopper – disk powder system set to a PFR of 16.2 g/min. The normalized results are shown in Fig. 6. It is observed that middle region of powder splitter travel was relatively linear, so the PFR in 0.2° increments was measured in the 14–16° area. After normalizing the data, the finest resolution achieved was approximately 1.44% of the maximum PFR per 0.2° increment in the middle, linear region. Thus, for a 16.2 g/min maximum PFR the resolution is approximately 0.2 g per 0.2°

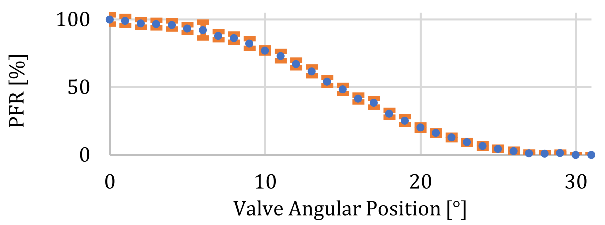

Fig. 6. Normalized PFR resolution curve for DPSS.

Further calibration of the valve was performed with the existing powder system set to deliver a maximum PFR of 50.0 g/min for the cladding tests discussed in Section 3.4. Normalizing the higher PFR results indicated that the original PFR resolution curve is applicable to higher PFR into the valve.

Endurance tests have also been performed to evaluate the effect of powder splitter wear on PFR resolution after prolonged use. The valve was set to rotate from open to closed in 5 s intervals with 30.0 g/min of powder flowing through. After 190 h of testing, the resolution has remained within the range of 0.42 – 0.49 g/min per 0.2° increment.

3.2. Response time

The time response of the DPSS was measured using an electronic scale to observe the time between no powder flow and full powder flow through the valve. Specifically, the valve time response was defined as the time between when the valve servo motor received a signal to move the splitter and when the PFR from the outlet of the valve reached a steady state. Five identical time response tests were performed, Fig 7.

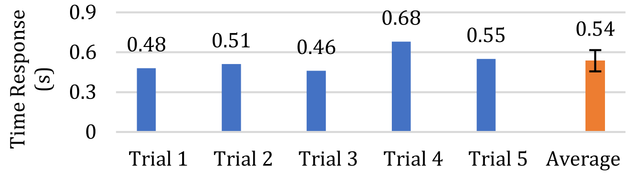

Fig. 7. Electronic scale time response data for DPSS.

The voltage from the dynamic mass scale is shown in Fig. 8. PFR reaches steady state in <1 s. The delay is due to a small motor signal delay and the powder travelling through the valve channels and approximately 200 mm of tubing before reaching the scale. Thus, if a look-ahead function could determine when PFR needs to be manipulated, the DPSS can be activated beforehand to make up for the overall time response delay.

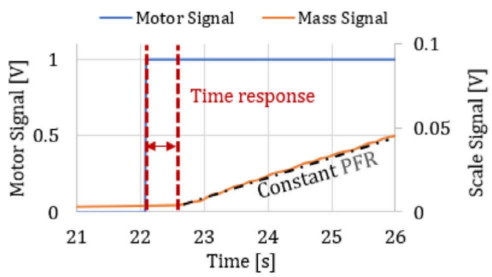

Fig. 8. Example of electronic balance time response test.

3.3. Single-Line cladding time response tests

The DPSS was installed on the DMG Mori Lasertec 65 3D hybrid, Fig. 9, and time response tests were performed during DED cladding. A single-line clad was deposited while the valve switched the PFR between two predetermined values, which resulted in two different clad heights. Predetermined values are defined in percentage of the total powder splitter angular range of motion, not percentage of maximum PFR for this experiment because only the change in clad height needed to be considered. Since the laser feed rate (mm/min) is known, the time response was determined by dividing the length of the transitional region between two clad heights and by the laser feed rate.

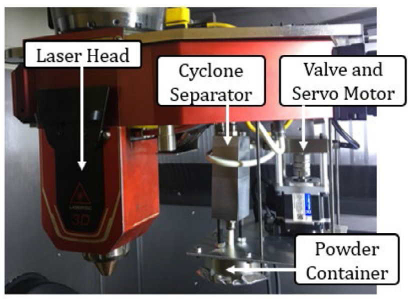

Fig. 9. DPSS prototype setup in DMG Mori Lasertec 65 3D hybrid.

Three PFR transition settings were tested: 100%–25%, 100%–50%, and 100%–75%. The clad geometry of the 100% - 25% transition is shown in Fig. 10. The laser feed rate was set to 1000 mm/min and the PFR was switched at an interval of 2 s.

It was found that the time response from a partially open (e.g. 25%, 50%, etc.) to a fully open (i.e. 100%) position was typically faster than the time response from a fully open to partially open position,

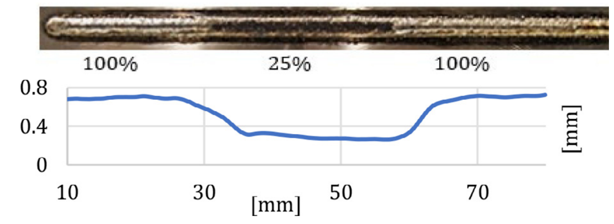

Fig. 10. Example cladding time response test with valve switching from 100% open to 25% open.

Fig. 11. This may be due to a small delay in the recovered argon reaching the laser head when switching valve positions. However, even with this delay, the difference between both responses are within 0.2 s. Additionally, it was observed that smaller valve rotations resulted in shorter response times.

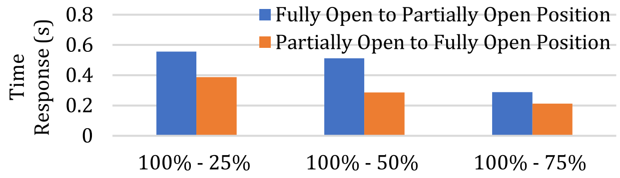

Fig. 11. Average time response for single-line cladding tests for laser feed rate = 1000 mm/min.

3.4. Energy/Powder-Controlled deposition with developed dpss

A thin wall deposition was also performed to demonstrate a new application of the increased PFR control bandwidth. As referenced in Section 1.2, interpass dwells of 5 s or longer are often used as a meltpool energy management technique, but this approach significantly increases the overall cycle time. To manage the energy accumulation without a long dwell time, *EF* may be decreased by lowering the laser power while holding laser feed rate constant as the DED cycle progresses. However, *EF* can also be decreased via an increase in laser feed rate while maintaining laser power, per (1) [3]. Increasing laser feed rate to manage heat accumulation reduces the cycle time.

When this unique feed-based energy management approach is used, *PF* is kept constant by increasing *PFR* in (2) to maintain a constant clad height for a stable DED process. For this test, the interpass dwell was reduced to 2 s to improve productivity. The 2 s dwell required the implementation of the DPSS to quickly change PFR between layers, which was not possible with the existing hopper – disk powder delivery system alone.

Using a numerical model of energy accumulation during a DED build of a 32-layer thin wall, a set of *EF* values were estimated to maintain overall meltpool energy constant. From the *EF* values five pairs of PFR and laser feed rate values (Table 1) were derived from (1) and (2) for the layers of the 32-layer thin wall. Consulting Fig. 6, using a starting PFR of 50.0 g/min yielded approximately a 0.75 g/min resolution per 0.2° in the linear region.

Table 1
Calculated PFR and laser feed rate pairs for constant PF.

PFR (g/min)	23.5	28.0	32.5	37.0	43.5
Feed (mm/min)	1000	1200	1400	1600	1850

A comparison of a thin wall created with feedrate based energy control (right) and a thin wall deposited with no energy control (left) is shown in Fig. 12. The average thickness for cross sections normal to the deposition direction confirm that meltpool energy management when depositing thin walls results in a more stable process by producing a constant clad width. Additionally, the thin wall created using feedrate based energy control had a height of 23.8 mm compared to the programmed height of 22.4 mm. Considering that an overbuilt geometry is better than underbuilt for DED process stability and post-processing purposes, the results using the DPSS for energy control is much more desirable. More importantly, deposition time was improved from 48 s with no control to 32 s with the energy/powder control. Overall, the DPSS allowed for more productive DED than would be possible with the existing powder delivery system.

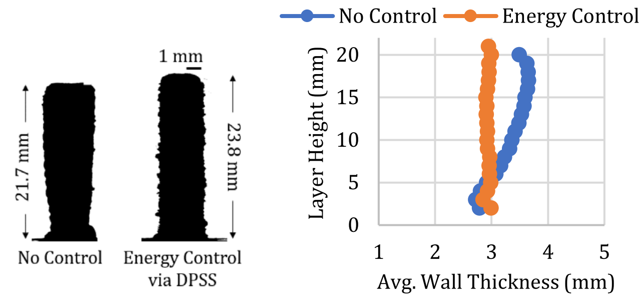

Fig. 12. No control vs. energy control via DPSS thin wall comparisons.

4. Conclusion

The developed DPSS is a solution for quickly controlling PFR for DED. It is placed in series with the powder feeding system, as close to the laser head as possible to decrease the PFR control time as compared to the existing powder delivery system alone.

A variety of tests were performed to determine the capabilities of the DPSS: PFR stability, PFR resolution, electronic scale time response, single-line cladding time response, and an energy/powder-controlled thin wall deposition. Results demonstrated that powder flow stably travelled through the DPSS, the valve's PFR resolution, and the time response of changing PFR, which was found to be approximately 0.5 s.

Cladding test results show that the time response of the DPSS system is capable of compensating for clad height inconsistencies using a control system. Future research includes more endurance tests and designing a PFR sensor for feedback control based on the user's defined PFR and/or for look-ahead capabilities.

By decreasing the PFR change time response, the DPSS allows for changing clad height quickly for different features and potential for a control system to compensate for clad height inconsistencies. Additionally, the unused powder is rerouted to a recycling container increasing the powder efficiency of DED cycles with interpass dwells. The DPSS allows for DED to be a more productive, efficient, and advanced manufacturing process.

References

[1] Soshi M, Odum K, Li G (2019) Investigation of Novel Trochoidal Toolpath Strategies for Productive and Efficient Directed Energy Deposition Processes. *CIRP Annals Manufacturing Technology* 68(1):241–244. https://doi.org/10.1016/j.cirp.2019.04.112.
[2] Thompson SM, Bian L, Shamsaei N, Yadollahi A (2015) An Overview of Direct Laser Deposition for Additive Manufacturing; Part I: Transport Phenomena, Modelling and Diagnostics. *Additive Manufacturing* 8:36–62. https://doi.org/10.1016/j.addma.2015.07.001.
[3] Fujishima M, Oda Y, Ashida R, Takezawa K, Kondo M (2017) Study on Factors for Pores and Cladding Shape in the Deposition Processes of Inconel 625 by the Directed Energy Deposition (DED) Method. *CIRP Journal of Manufacturing Science and Technology* 19:200–204. https://doi.org/10.1016/j.cirpj.2017.04.003.
[4] de Oliveira U, Ocelik V, De Hosson JThM (2005) Analysis of Coxial Laser Cladding Process Conditions. *Surface and Coatings Technology* 197(2-3):127–136. https://doi.org/10.1016/j.surfcoat.2004.06.029.
[5] Arrizubieta JI, Martinez S, Lamikiz A, Ukar E, Arntz K, Klocke F (2017) Instantaneous powder flux regulation system for Laser Metal Deposition. *Journal of Manufacturing Processes* 29:242–251. https://doi.org/10.1016/j.jmapro.2017.07.018.
[6] Shepherd CB, Lapple CE (1939) Flow Pattern and Pressure Drop in Cyclone Dust Collectors. *Industrial and Engineering Chemistry* 31(8):972–984. https://doi.org/10.1021/ie50356a012.
[7] Leith D, Mehta D (1973) Cyclone Performance and Design. *Atmospheric Environment* 7(5):527–549. https://doi.org/10.1016/0004-6981(73)90006-1.
[8] Wang L, Parnell CB, Shaw BW, Lacey RE (2006) A Theoretical Approach for Transactions of the ASABE, 49/2:491–503, DOI: 10.13031/2013.20404.